

A search for magnetic fields around disk-like galaxies at $z \sim 0.5$

Anna Williams*^a †, Britt Lundgren^b, Sui Ann Mao^c, Eric Wilcots^a, Don York^d, and Ellen Zweibel^a

^aDepartment of Astronomy, University of Wisconsin - Madison, Madison, WI, USA; ^bDepartment of Physics, University of North Carolina-Asheville, Asheville, NC, USA; ^cMax-Planck-Institut für Radioastronomie, Bonn, Germany; ^dDepartment of Astronomy & Astrophysics, University of Chicago, Chicago, IL, USA

E-mail: williams@astro.wisc.edu

Magnetic fields are ubiquitous in the universe. They accelerate cosmic rays, affect star formation, and regulate the redistribution of matter and energy within galaxies. Despite their prevalence, the origin and growth of magnetic fields is not well understood. We present the preliminary results of a Faraday rotation measure survey that aims to determine whether the environments of young, disk-like galaxies at redshift $z \sim 0.5$ contain large-scale magnetic fields. Our survey contains 38 quasars with SDSS identified MgII absorption systems at $z \sim 0.5$, and over 100 quasars that serve as controls to constrain the contributions from both the foreground rotation measure and the intrinsic rotation measure of the quasar. We utilize the broadband, polarization capabilities of the S-band receiver at the Karl G. Jansky Very Large Array to simultaneously observe Stokes I, Q, U, and V from 2-4 GHz. This large wavelength coverage allows us to use multiple methods of constrain the Faraday rotation, including rotation measure synthesis, and fractional QU -model fitting. We present the initial results of the survey, including new polarization detections and rotation measures.

EXTRA-RADSUR2015 (*)
20–23 October 2015
Bologna, Italy

(*) This conference has been organized with the support of the Ministry of Foreign Affairs and International Cooperation, Directorate General for the Country Promotion (Bilateral Grant Agreement ZA14GR02 - Mapping the Universe on the Pathway to SKA)

*Speaker.

†This research was supported by the Center for Magnetic Self-Organization in Laboratory and Astrophysical Plasmas which is a Physics Frontier Center established by the National Science Foundation (NSF), the National Space Grant College and Fellowship Program, and the Wisconsin Space Grant Consortium. Travel support was also provided by the Bautz Travel Fellowship from the University of Wisconsin and the American Astronomical Society International Travel Grant through the NSF.

1. Introduction

Magnetic fields are ubiquitous in the universe, spanning many orders of magnitude in scale-length and strength in all astrophysical phenomena. On the smallest and most local scales, the Earth's dipole magnetic field protects life from harsh, gene-altering high energy particles in the solar wind. Stars also have dipole magnetic fields that can get wrapped up and twisted by differential rotation, causing the formation of star spots and prominences. Within the interstellar medium (ISM), magnetic fields affect the turbulent properties of the gas and star formation. These magnetic fields accelerate and confine cosmic rays, which in turn play important roles in the dynamics and energy balance of the ISM. Large-scale spatially ordered magnetic fields are found in between the spiral arms of face-on galaxies and to extend vertically above and below disks of edge-on galaxies. On the largest scales, magnetic fields play a fundamental role in radio jets and lobes, and permeate the intracluster medium.

Despite their pervasiveness, the origin and growth of magnetic fields is still not well understood. Some of the outstanding questions around magnetic fields include:

1. *How and when did the first magnetic fields form in the universe?*
2. *How do the strength and structure of magnetic fields evolve with redshift?*
3. *(How) Do magnetic fields affect astrophysical processes that in turn define the evolution of galaxies?*
4. *Are there magnetic fields in the IGM? If so, how did they get there and what are their strengths?*

Until we know the answers to these questions, our understanding of the cosmological evolution of the universe will be incomplete. While theory and simulations continue to improve our knowledge of the dynamo processes key to the production of magnetic fields, the real advancement comes when we compare these results to actual observations. Recent upgrades to available radio telescopes provide us with simultaneous wide-band polarization coverage, and are revolutionizing the way we observe magnetic fields.

1.1 Observing magnetic fields in distant galaxies

Since magnetic fields do not emit radiation, we rely on observing the light emitted by baryons interacting with the fields. There are four observational tools available for measuring astrophysical magnetic fields: synchrotron emission, polarized emission or absorption from magnetically aligned dust grains, Zeeman splitting, and Faraday rotation. Of all of these tracers, Faraday rotation is the most powerful when trying to probe magnetic fields at greater distances.

Faraday rotation, or rotation measure (RM), is due to the birefringence property of magnetized plasma which causes the plane of polarization to rotate as a function of wavelength. This is described by

$$\Delta\theta = \lambda^2 0.812 \int_{source}^{observer} n_e B dl = \lambda^2 RM.$$

Here, $\Delta\theta$ is the change in angle of linear polarization in rad, λ^2 is the wavelength of observation squared in m^2 , n_e is the electron density in cm^{-3} , B is the strength of the line of sight magnetic field in μG , dl is the distance traveled by the emission in pc, and RM is the Faraday rotation in $rad\ m^{-2}$.

In principle, the magnetic field strength can be determined by measuring the change in polarization angle across different wavelengths, and obtaining information about the electron density and path length. In practice, it is a bit more complicated since the measured RM is the sum of *all* RM contributions along the line of sight. If there is linear polarized emission from a QSO, Faraday rotation will occur if the sightline to the QSO passes through a magnetized medium. Our own galaxy contains magnetic fields, so it will contribute to every observed RM. Intervening galaxy discs or halos, intergalactic medium, intracluster gas, and gas associated with the QSO may all contribute to the RM (see Figure 1). This makes it very difficult to discern the RM associated with each component along any single sightline. To overcome this and isolate Faraday rotation associated with a particular component along the line of sight, large, well designed RM surveys are needed.

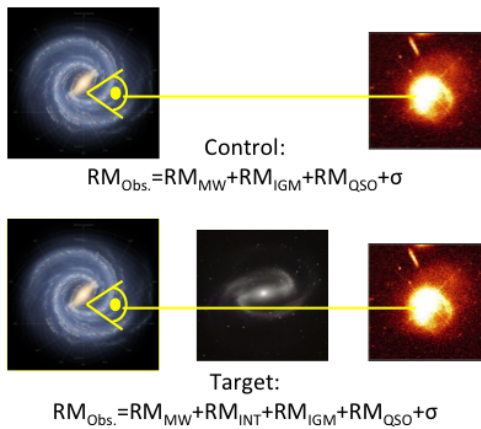


Figure 1: Examples of sightlines to distant QSOs. The top sightline is an example of an ideal control QSO with no intervening extragalactic systems contributing to the observed RM ($RM_{Obs.}$). The only components along the line of sight are the Milky Way (RM_{MW}), intergalactic medium (RM_{IGM}), gas associated with the QSO (RM_{QSO}), and the uncertainty (σ). The bottom sightline is an example of an ideal target QSO. In this case the $RM_{Obs.}$ also contains the RM associated with the intervening galaxy (RM_{INT}).

Early efforts to measure the evolution of magnetic fields using Faraday rotation were pioneered by Kronberg, Perry, and collaborators [12]. During the 1980's and early 1990's they found hints that QSOs with absorption lines may exhibit excess RM due to intervening extragalactic systems. Using a small sample, Oren and Wolfe [14] found that QSOs with damped Lyman- α were more likely to have excess RM than QSOs without such strong absorption features.

More recently, Bernet et al. [1, 3] found that QSOs have larger $|RM|$ if they have strong MgII absorption and closer impact parameters to the presumed absorber. Farnes et al. [8] compiled polarization data from all available radio surveys, and showed that QSOs with flat radio spectra and MgII absorption tend to have larger $|RM|$ than QSOs with steep radio spectra or without MgII absorption. Flat-spectrum sources are associated with core-dominated QSO, and can be used as a proxy for identifying a source likely to have an optical counterpart. Therefore, these authors concluded that the excess RM detected in flat-spectrum QSO with MgII absorption is due to magnetic fields in the intervening system. While these results give tantalizing hints that MgII absorbers host coherent fields, their interpretation is hampered by the heterogeneous nature of their samples, limited narrow-band data, and the general issue that we know little about how the background QSOs contribute to measurements of extragalactic RMs.

1.2 Why MgII absorption systems?

Absorption line studies of distant QSOs have found MgII absorption to occur in photo-ionized gas clouds with a neutral column density of $N(HI) \sim 10^{18} - 10^{22} \text{ cm}^{-2}$ [16] and a temperature

of $T \sim 10^4$ K [5]. These absorption lines are detected in the optical at $0.3 < z < 2$, and have been shown to typically arise in $\sim 0.5L_*$ intermediate-type galaxies [21]. The occurrence of MgII absorption has been found to correlate with a variety of other observables at various redshifts. At intermediate redshifts ($0.3 < z < 1$) there is evidence for a correlation between MgII equivalent width and galaxy star-formation rate [21], which agrees with observations of outflowing MgII at similar redshifts [17]. At lower redshifts $z < 0.1$, MgII has been found to trace infalling neutral gas feeding the host galaxy’s reservoir [11], and to generally arise in spiral galaxies with evidence of a minor mergers [6]. While Mg II absorbers may probe a wide range of astrophysical phenomena including gas in the disks and halos of galaxies, high velocity clouds, dwarf galaxies, or even galactic outflows, a synthesis of our current understanding of Mg II absorbers is that these systems provide an opportunity to understand the conditions in and around evolving galaxies.

2. A new survey in search of magnetic fields near evolving galaxies at $z \sim 0.5$

In light of the sheer complexity intrinsic to extragalactic RM studies and the upgraded capabilities of the VLA, we are conducting a new and carefully defined survey of QSO RMs that probe the MgII absorbing material surrounding galaxies at $z \sim 0.5$. The primary goal of our survey is to constrain when coherent magnetic fields arose in the universe by determining if young, disk-like galaxies at $z \sim 0.5$ have associated fields. As was done in a few previous studies, we have selected two samples of QSOs: a ‘control sample’ and a ‘target sample’ (see Figure 1). The sample selection design considers the results of previous surveys, and accounts for the unknown nature of the RMs intrinsic to QSOs. By utilizing the full wide-band coverage offered by the Karl G. Jansky Very Large Array (VLA) at S-band (2-4GHz), we are able to implement multiple advanced tools like RM synthesis [4] and QU -fitting [15] to determine more robust RMs than was possible with the limited wavelength coverage of previous surveys. S-band also avoids longer wavelengths (≤ 1.4 GHz) which are more susceptible to depolarization effects [19].

All of the QSOs in our survey were previously detected in the SDSS¹ and FIRST². We use a flux density cutoff of 4.5mJy at 1.4 GHz. This cutoff was determined so that we can detect weakly polarized sources ($\sim 3\%$) within 30m of integration ($\text{RMS} \sim 10\mu\text{Jy}$). We impose a cutoff in galactic latitude such that all QSOs in our survey are located off the Galactic midplane, $|b| > 50^\circ$, to avoid large Faraday rotation contribution from the Milky Way [18].

The target sample consists of 38 radio QSOs that have only one MgII absorption line in their SDSS spectra. While this does not guarantee the absence of additional intervening sources of RM along the line of sight, it minimizes the chances of such an occurrence. The QSOs were also selected because there is a photometric detection of an intervening galaxy in the SDSS. The intervening galaxy must have a photometric redshift matching the redshift of the MgII absorption in the QSO spectrum. This limits the redshift range of the MgII absorption to $0.38 < z < 0.65$. We also restricted the separation between the QSO and the photometrically detected intervening galaxy to $D < 150$ kpc (e.g., Figure 2). This distance cutoff was generated by taking into account that Bernet et al. [3] found that MgII absorbing galaxies with impact parameters $D < 50$ kpc were more likely to have $|\text{RM}| > |\text{RM}_{\text{MW}}|$. Our range in impact parameters will allow us to test the [3] results, while

¹Sloan Digital Sky Survey

²VLA Faint Images of the Radio Sky at Twenty-Centimeters

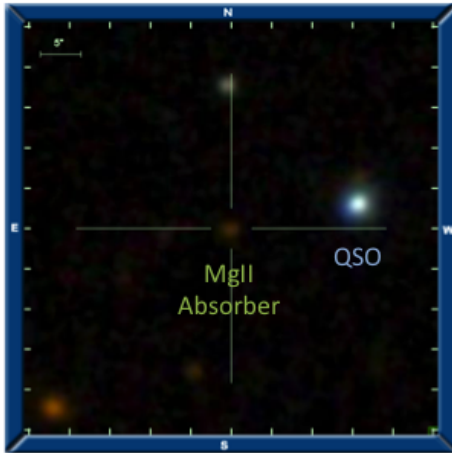


Figure 2: Example of SDSS photometric detection of MgII absorber. The image is centered on a galaxy that has a photometric redshift that matches the spectroscopic redshift of the MgII absorption line detected in the SDSS spectrum of the QSO on the right.

also increasing the sample size of MgII absorbers. Half of the sample, or 19 of the target QSOs, have $D < 50\text{kpc}$, and only 7 have $D > 100\text{kpc}$. While this sample is not much larger than the 28 strong MgII absorption systems analyzed by [3], it is more refined. Unlike [3], our target sample QSOs only contain one MgII absorption feature in their SDSS spectra and the MgII absorbers span a much narrower range in redshift (only 12 of the objects in [3] would meet our selection criteria).

The control sample consists of 112 radio QSOs that match our target sample in every way *except* for MgII absorption. Thus, our control sample has distributions in luminosity, redshift, and right ascension that closely match our target sample. While the most recent large studies of extragalactic RMs do not find a definitive change of RM with QSO redshift [9, 8], our selection strategy will allow us to statistically account for the possibility that some of the observed Faraday rotation could arise in the radio source itself or in its local environment. The right ascension requirement minimizes the overhead needed for calibration observations, and improves the efficiency of our survey. This also has the added benefit of increasing the density of known RMs in the direction of our survey which is likely to improve our estimates of the RM_{MW} .

3. Preliminary Results

The survey was conducted during the 2014A and 2015A observing semesters at the VLA, and the observations were completed in September 2015. Observations were carried out in both A and BnA configurations, which gives us strong resolving power to morphologically study and identify the physical processes at work in the QSO. Data were taken at S-band (1.988-4.014 GHz) in 16 spectral windows, each containing 64 2-MHz channels. We are still in the process of calibrating and reducing the data using CASA³. At this time, we present the preliminary results for one of the QSOs in the control sample.

Figure 3 is an integrated total intensity, phase-center image of one of the control QSOs, Obj 00. The image has an RMS of $15\mu\text{Jy beam}^{-1}$ and restoring beam of $1.2'' \times 0.7''$. In addition to detecting the control QSO, we detect 6 additional sources. They are all circled and labeled in magenta. White contours show total intensity at 1.4 GHz taken from the NVSS⁴, and that 3 sources including the

³Common Astronomy Software Applications, <http://casa.nrao.edu>

⁴National Radio Astronomy Observatory VLA Sky Survey

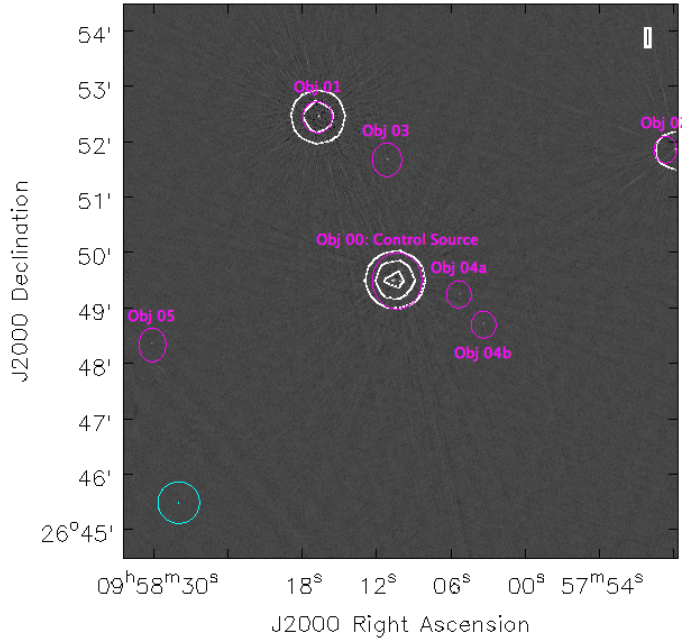


Figure 3: VLA Stokes I image at S-band illustrating both the high resolution and wide-field capabilities of our survey. The grayscale image is a total intensity map integrated across 2-4GHz from our recent observations. White contours are produced from NVSS. Magenta circles highlight sources detected in total intensity. The beam sizes are illustrated in cyan in the lower left. The inner circle (or dot in this scale) is $1.2'' \times 0.7''$ representing the beam of our 2-4GHz observations, and the outer circles is $45''$ representing the NVSS beam.

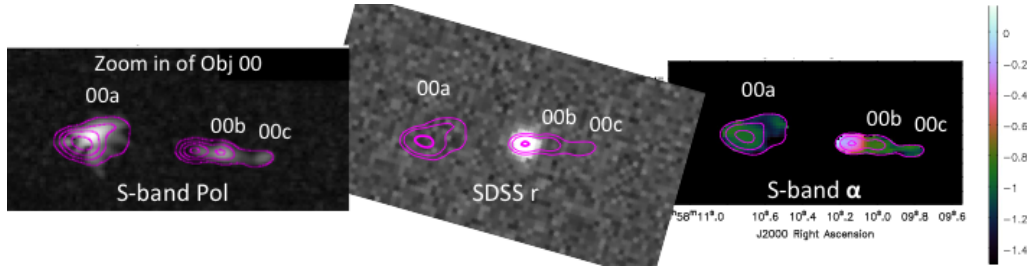


Figure 4: Three zoomed in images of control source Obj 00 from Fig. 3. In each zoom-in the magenta contours trace the total intensity of the VLA observations integrated across the entire S-band, 2-4GHz. The left image shows the polarization in greyscale. The middle image shows the SDSS r-band image in greyscale, and the right image shows the spectral index, α where $S_\nu \propto \nu^\alpha$, as described by the colorbar.

control QSO were previously detected. When compared to FIRST, we found that all sources except for Obj 04a were previously detected. The dimensions of this figure were chosen in order to image out to $\sim 80\%$ power of the primary beam (Obj 02 is just outside 80% power). This field of view was found by Jagannathan [10] to be reliable for accurate polarization measurements. Beyond this limit the uncertainty in the direction dependent instrumental polarization becomes too large, and the polarization should not be trusted until corrections are implemented.

A zoom in of the control QSO is shown in Figure 4. The left greyscale image shows the polarized intensity at S-band ($\text{RMS} = 20 \mu\text{Jy}$), the middle greyscale image is the SDSS intensity map at r , and the right image and corresponding colorbar show the spectral index, α , across the source. All three images show the S-band total intensity contours overplotted in magenta. The three brightest points of polarization have been labeled 00a, 00b, and 00c in descending polarized intensity. Several interesting results can be seen in this figure. First of all, as intended, the high resolution VLA observations are resolving structure in the QSO. The combination of the high resolution and simultaneous broad wavelength coverage of S-band allow us to map α across the

Table 1: Preliminary results after imaging

Object	SDSS z	α	P^a	P S/N	$\% P$	RM_{obs}^b		NVSS P^a	NVSS $\% P$	NVSS RM_{obs}^b
00a	1.5	-0.98	0.88	49	19.5%	+33 ± 2.5		3.88 ± 0.24	4.01%	+44.1 ± 13.1
00b	1.5	-0.82	0.36	20	12.2%	+30 ± 5.5		3.88 ± 0.24	4.01%	+44.1 ± 13.1
00c	1.5	-1.05	0.19	10	19.5%	+40 ± 10.6		3.88 ± 0.24	4.01%	+44.1 ± 13.1
01	0.678 ^c	-1.12	0.12	6.8	0.6%	+141 ± 16.3				
02	(?) ^c	+0.13	0.12	6.7	1.0%	+6 ± 16.5				
03	0.317	-0.64	0.08	4.6	6.3%	+44 ± 25.0				

Notes:

^a Polarized intensity in mJy beam⁻¹. The noise in the recent S-band VLA observations is ± 0.020 mJy beam⁻¹.^b RMs in rad m⁻².^c These sources did not have a direct optical detection in SDSS.

source. Based on the map of α , the QSO appears to be resolved into a flat- α core with a steep- α lobe on either side. As expected, this flat- α core is coincident with the SDSS detection. We can also see that the peaks in polarization are coincident with steeper- α . Note the strange, star-like structure visible in the polarized intensity map is likely an artifact of imaging and RM synthesis. Further examination will need to be done to correct this effect in the future.

We also detect polarization in three sources that were previously not known to be polarized. A summary of the measurements is given in Table 1. Object labels are listed in column (1), followed by their SDSS redshift in column (2). The values listed in the following five columns (3-7) were all taken at the pixel with the greatest polarization in the source. This includes the spectral index (α), polarized intensity (P), signal to noise of the polarized intensity (P S/N), degree of polarization ($\%P = P/I$), and the rotation measure determined via RM synthesis (RM_{obs}). The last three columns note the previous polarization measurements available for the sources in this field. Our 7min observation produced polarization measurements an order of magnitude deeper than previously available with the NVSS.

4. Conclusion

A preliminary examination of our data shows that our survey will provide new and interesting insights into the structure and evolution of QSOs while advancing the study of magnetic field evolution in galaxies. As intended, our observations are capable of resolving structure in distant QSOs, and the wide bandwidth provided by the VLA allow us to determine the spectral index and RM across the entire object. For the source that was previously detected in polarization (Obj 00) in the NVSS, we find that our RM estimates agree with previous results, and verify that our RM analysis method is valid. As predicted, we detect a greater degree of polarization ($P\%$) at S-band

than at L-band, but a more detailed examination will need to be done to see if we are missing flux due to the lack of short spacings.

Despite not being able to correct for direction dependent instrumental polarization, our survey detects new polarized sources within 80% power of the primary beam. These serendipitous discoveries will be excluded from the analysis of the intended survey until ancillary data is assembled for identification. However, they may prove useful in estimating the RM_{MW} . The current best RM catalog available for estimating the RM_{MW} only has ~ 1 source per square degree [20]. Fluctuations in RM may occur on scales as small as $6''$ [7], so the addition of RM sources near our QSOs of interest will increase the fidelity of RM_{MW} estimates. These new detections show the power of the upgraded VLA to detect polarization at S-band.

The final results of this survey will help to constrain the occurrence of coherent magnetic fields around young, evolving galaxies at $z \sim 0.5$. The methods and techniques used in our survey will pioneer similar types of studies to be done with data from the VLA Sky Survey and the Square Kilometer Array. We are entering a new era of radio polarization observations that will provide opportunities to answer outstanding questions about the origin and evolution of magnetic fields.

References

- [1] Bernet, M. L., et al. 2008, *Nature*, 454, 302
- [2] Bernet, M. L., Miniati, F., & Lilly, S. J. 2010, *ApJ*, 711, 380
- [3] Bernet, M. L., Miniati, F., & Lilly, S. J. 2013 *ApJ*, 772L, 28
- [4] Brentjens, M. A. & de Bruyn, A. G. 2005, *A&A*, 441, 1217
- [5] Charlton, J. C., et al. 2003, *ApJ*, 589, 111
- [6] Churchill, C, Kacprzak, G. G., & Steidel, C. 2005, *IAU 199* (Cambridge University Press)
- [7] Gaensler, B. M., et al. 2005, *Sci*, 307, 1610G
- [8] Hammond, A. M., Robishaw, T., & Gaensler, B. M. 2012, arXiv:1209.1438v3
- [9] Farnes, J. S., et al. 2014 *ApJ*, 795, 63
- [10] Jagannathan, P., et al. 2015, *AAS Meeting Abstracts*, 225, 336.31
- [11] Kacprzak, G. G., et al. 2011, *ApJ*, 733, 105
- [12] Kronberg, P. P. & Perry, J. J. 1982, *ApJ*, 263, 518
- [13] Kulsrud, R. M. & Zweibel, E. G. 2008, *RoPP*, 71, 046901
- [14] Oren, A.L. & Wolfe, A.M. 1995, *ApJ* 445, 624
- [15] O'Sullivan, S. P., et al. 2012, *MNRAS* 421, 3300
- [16] Rao, S. M., et al. 2011, *MNRAS*, 416, 125
- [17] Rubin, K. H. R., et al. 2010, *ApJ*, 719, 1503
- [18] Schnitzeler, D. H. F. M. 2010, *MNRAS*, 409, L99
- [19] Schnitzeler, D. H. F. M., Banfield, J. K., & Lee, K. J. 2015, *MNRAS*, 450, 3579
- [20] Taylor, A. R., Stil, J. M., & Sunstrum, C. 2009, *ApJ*, 702, 1230
- [21] Zibetti, S., et al. 2007, *ApJ*, 658, 161